

Dynamics and Sensitivity of Fractional-Order Delay Differential Model for Coronavirus (COVID-19) Infection

Fathalla A. Rihan^{1,*} and Velmurugan Gandhi²

¹ Department of Mathematical Sciences, College of Science, United Arab Emirates University, Al Ain, 15551, UAE

² Research Centre of Wind Energy Systems, Kunsan National University, Gunsan, South Korea

Received: 19 Jan. 2020, Revised: 1 Apr. 2020, Accepted: 12 Apr. 2020

Published online: 1 Jan. 2021

Abstract: In this paper, we provide a fractional-order delay differential model for *coronavirus* (CoV) infection to give us best understand what causes the intensity of symptoms and illness of contaminated lung and respiratory system. A fractional-order and time-delays are incorporated in the model to naturally represent the effects of both long-run and short-run memory in the dynamics of cells and tissues of immune system. Some interesting sufficient conditions that ensure the asymptotic stability of the steady states are obtained. Sensitivity analyses such as sensitivity to variations in the rate of interferon, rate of innate immunity cells, rate of adaptive immunity cells, and variation in pathogen virulence are investigated to provide insight into the role of each and most effective parameter of the model. This consideration may deliver experiences into respiratory infections and define the foremost compelling parameters for treatment.

Keywords: Coronavirus, Delay differential models, Fractional calculus, Immunological barrier, Infectious disease, Sensitivity

1 Introduction

The ongoing pandemic coronavirus (CoV) disease (COVID-19) outbreak was first reported in Wuhan, China, in December 2019 and has spread to more than 197 territories Worldwide. WHO declared COVID-19 as pandemic on 11 March 2020. This rising infectious disease involves a fast spreading, endangering the health of huge numbers of people. Thus requires immediate actions have to be taken to prevent the disease at the community level. COVID-19 is the seventh member of the coronavirus (CorV) family, together with MERS-CoV and SARS-CoV, that can spread to humans [1]. The symptoms of the infection include fever, cough, shortness of breath, and diarrhea. In more severe cases, it causes respiratory illness ranging from mild disease to severe disease and death. However, some people infected with the virus never develop symptoms [2]. The incubation period of COVID-19 is between 3–14 days or longer. While incubation time for flu is 1-3 days [3]. During the period of latent infection, the disease may still be infectious. The virus is very series can spread fast from person to person through respiratory droplets and close contact [4]. Therefore, many researchers and scientists are interested to know how to create treatment methods against such infectious diseases. Those methodologies help to partially understand the complexity of the dynamics/interactions between specific viral or bacterial pathogens and the human host. The community of mathematical modelers has been addressing specific aspects of infectious diseases for a long time [5,6]. Most of these efforts have focused on multi-level diseases and adopted quite different computational approaches [7,8,9,10,11]. In [8], the authors considered epidemiological models with nonlinear incidence rates and examined the dynamical behaviors of the considered model. In [11], the author discussed the developments and importance of the mathematical modeling to understanding of HIV infection.

The transmission COVID-19 at the cells level may cause upper-respiratory-tract infection among humans. In human cells, we have healthy, infected, virus cells and antibodies that could be considered as input parameters and the output will be infected lung cells. Accordingly, the characteristics of COVID-19 tend to be similar to SARS-CoV. This will help us to determine some routes of infection and prevent its spread. Moreover, the immune response system of human plays a vital role in the protection against dangerous infections [12,13,14]. In the view of biological systems, the stimulation of the

* Corresponding author e-mail: frihan@uaeu.ac.ae

defensive immune responses suggests that the kinetics of innate immune responses critically impinge on the development of pathogen-specific adaptive immune responses. In [15], the authors investigated the dynamics of influenza A virus infection model with a human immune response. Also, the immune response to hepatitis B virus infection was discussed in [16]. Many research papers discussed transmission of CoV among groups [17, 18, 19]. However, the dynamics of CoV infection are not intensively addressed in an individual (organism), in the literature, which we investigate in the present paper.

In the literature, most scientific modeling of biological systems with memory is based either on delay differential equations (DDEs) with integer-order or fractional-order differential conditions without a delay [20]. However, fractional-order calculus is more suitable than integer order ones in modeling biological systems with intrinsic memory and long-range interactions such as epidemic evolution systems [5]. Modeling such frameworks using fractional-order differential conditions has more points of interest than classical integer-order scientific modeling, in which the impacts of memory or long-range intuitive are dismissed [21, 22, 23]. In fact, memory effects play an essential role in the spread of diseases. Moreover, fractional-order derivatives of the model provide more accurate and generalized results than the integer-order derivatives. Fractional-order models have both memory and nonlocality effects which are rather relevant to epidemic spread. Therefore, many researchers have focused their interest on investigating the dynamics of fractional-order epidemic models in recent decade [24, 25, 26, 27, 28, 29]. The problem of stability and Hopf bifurcation of fractional-order delayed Ebola virus infection model with cytotoxic T-lymphocyte (CTL) response have been investigated in [26]. In [29], the authors have examined the dynamical behaviors of considered fractional-order model Hepatitis-C Virus model in presence of interferon- α treatment. Recently, Rihan and Velmurugan in [30] proposed a delay differential model with fractional-order for tumor immune system with external treatments. They investigated the necessary and sufficient conditions for stability of the steady states and Hopf bifurcation with respect to two different tumor time-delays. A fractional-order model of cytotoxic T lymphocyte response with long-term behavior of tumor growth and with tumor elimination has been investigated in [31].

The present paper aims to propose a compartmental mathematical model with fractional-order and time-delay for the dynamics of viral infection of COVID-19 and immune system (in an individual), with respiratory infections. This may help us better understand what causes the intensity of symptoms, infectivity of the virus and the host, and duration of the disease. Parameters of system dynamics models are subject to uncertainty. Sensitivity analyses are conducted to provide insight into how uncertainty in the parameters affects the model outputs and which parameters tend to drive these variations. Herein, we study sensitivity of the model to small changes in its parameters to evaluate how the severity of infection can be affected by disturbing the parameters. Sufficient conditions that ensure asymptotically stable of existing steady states, using Laplace transform and characteristic roots, are also deduced. The rest of the manuscript is structured as follows: In Section 2, we provide a fractional-order delayed model for the dynamics of CoV with immune response. In Section 3, we investigate the qualitative feature of the model and deduce some conditions which guarantee the asymptotic stability of the steady states. Sensitivity analysis with numerical simulations are discussed and provided in Section 4. Discussion and conclusion are presented in Section 5.

2 Dynamics of COVID-19 infection

In fact, the immune system has two types of immunity: innate immunity and adaptive immunity. During viral infections, the adaptive immune response plays a significant role in the control of infection process. This response is generated by two arms of immunity. The first one based on antibodies, called humoral immunity, is programmed to eradicate viral pathogens, while the second one mediated by Cytotoxic Lymphocytes Cells (CTL), called cellular immunity, is programmed to destroy infected cells [32]. In the beginning of infection, the innate immune response develops first in minutes or hours, while adaptive immunity follows innate immunity occurs in days or weeks [33, 34]. The innate immune system uses receptors that are encoded by intact genes inherited through the germline [35], whereas the adaptive immune system uses antigen receptors [36]. Host cells are generated with counter components to distinguish virus-encoded molecular patterns and engender an antiviral reaction. Viral double-stranded RNA (dsRNA) is a well-characterized pathogen-associated molecular pattern recognized by cytosolic pattern recognition receptors retinoic acid inducible gene-1 (RIG-1), melanoma differentiation-associated protein 5 (MDA5), and endosomal toll-like receptor 3 (TLR3), resulting in type 1 interferon (IFN1) production [37]. Viruses utilize a unique evasion mechanism by synthesizing proteins that hinder the IFN1 production and secretion pathways. For instance, influenza A virus uses non-structural protein 1 to bind dsRNA [38], inhibiting RIG-1-like receptors and TLR3-dependent IFN1 synthesis. Dengue virus, on the other hand, prevents IRF3 phosphorylation through the non-structural protein 2B3 protease complex [39].

Similar to MERS-CoV and SARS-CoV, COVID-19 implements a mechanism to evade dsRNA sensors including RIG-1, MDA5, and endosomal TLR3 of the host immune system. Some studies have found that MERS-CoV and SARS-CoV

are sensitive to IFN1 treatment [40,41,42]. This viral interference in the host innate immune pathway enhances virus-induced disease progression and elevates the mortality rate to 60%. Antigen presenting cells (APC) are also essential in the induction and amplification of the human immune response [43].

2.1 Mathematical model

Herein, we provide a mathematical model, governed by a system of fractional-order delay differential equations, for the dynamics of COVID-19 infection with human immune response. The model variables have the following sense:

- $V(t)$, concentration of free CoV (COVID-19) in 1 ml of mucous compartment (particle/ml) in an organism;
- $H(t)$, proportion of healthy cells (cell/ml);
- $I(t)$, proportion of infected cells (cell/ml);
- $M(t)$, activated antigen presenting cells per homeostatic level (cell/ml);
- $F(t)$, interferon per homeostatic level of macrophages (cell/ml);
- $R(t)$, proportion of resistant cells (cell/ml);
- $E(t)$, effector cells per homeostatic level (cell/ml);
- $P(t)$, plasma cells per homeostatic level (cell/ml);
- $A(t)$, concentration of antibodies per homeostatic level (molecule/ml);
- $S(t)$, antigenic distance (cell/ml);
- $D(t)$, concentration of damaged cells in 1 ml in the compartment of upper respiratory (cell/ml).

The model considers the following assumptions (see Figure 1): The epithelial respiratory cells are divided as healthy cells, $H(t)$, infected, $I(t)$, dead, $D(t)$, or safe/resistant to disease, $R(t)$. The total number of epithelial cells is expected to be steady (i.e. $H(t) + I(t) + D(t) + R(t) = 1$). It is accepted that the infection particles $V(t)$ connected with healthy cells $H(t)$ and taint them, and contaminated cells $I(t)$ discharge unused infection particles upon their passing. Replication of $H(t)$ cells causes reproduction and decrease the load of $D(t)$ cells. Moreover, the dead cells fortify the enactment antigen APC, $M(t)$. In this way, APC stimulate within the creation of intergalactic $F(t)$, effector cells $E(t)$ and plasma cells $P(t)$. The interferons are intermingle with healthy cells and alter over time to a safe state. The effector cells $E(t)$ end contaminated /infected cells. The plasma cells surrender antibodies $A(t)$ that deactivate infection particles. This deactivation is controlled by the antigenic compatibility $S(t)$ between CoV disease particles and antibodies right presently made by the substance. $S(t)$ tallies the comparability between antibodies and contamination particles.

Based on the attention of some interfaces between immune response system against CoV, and due to the fact that both time-delays and fractional-order play a vital role in biological systems with memory which gives more degree of freedom, we propose a fractional-order delayed differential model, which is based on Marchuk model [6]. The model takes the form

$$\frac{d^\beta V(t)}{dt^\beta} = \gamma_V I(t) - \gamma_{VA} S(t) A(t) V(t) - \gamma_{VH} H(t) V(t) - \alpha_V V(t) - \frac{a_{V1} V(t)}{1 + a_{V2} V(t)}, \tag{1a}$$

$$\frac{d^\beta H(t)}{dt^\beta} = b_{HD} D(t) (H(t) + R(t)) + a_R R(t) - \gamma_{HV} V(t) H(t) - b_{HF} F(t) H(t), \tag{1b}$$

$$\frac{d^\beta I(t)}{dt^\beta} = \gamma_{HV} V(t) H(t) - b_{IE} E(t - \tau) I(t - \tau) - a_I I(t), \tag{1c}$$

$$\frac{d^\beta M(t)}{dt^\beta} = (b_{MD} D(t) + b_{MV} V(t)) (1 - M(t)) - a_M M(t), \tag{1d}$$

$$\frac{d^\beta R(t)}{dt^\beta} = b_{RF} F(t) H(t) - a_R R(t), \tag{1e}$$

$$\frac{d^\beta F(t)}{dt^\beta} = b_F M(t) + c_F I(t) - b_{FH} H(t) F(t) - a_F F(t), \tag{1f}$$

$$\frac{d^\beta E(t)}{dt^\beta} = b_{EM} M(t) E(t) - b_{EI} I(t - \tau) E(t - \tau) + a_E (1 - E(t)), \tag{1g}$$

$$\frac{d^\beta P(t)}{dt^\beta} = b_{PM} M(t) P(t) + a_P (1 - P(t)), \tag{1h}$$

$$\frac{d^\beta A(t)}{dt^\beta} = b_A P(t) - \gamma_{AV} S(t) A(t) V(t) - a_A A(t), \quad (1i)$$

$$\frac{d^\beta S(t)}{dt^\beta} = rP(t)(1 - S(t)). \quad (1j)$$

Here, $\frac{d^\beta}{dt^\beta}$ is the fractional-order derivative, with $0 < \beta \leq 1$. From the above-mentioned assumption the dead cells $D(t)$ is

$$D(t) = 1 - I(t) - R(t) - H(t). \quad (1k)$$

The interacting parameters in the model (1a-1j) are provided in Table 1. The time-lag $\tau >$ is incorporated in the model to represent required time for reaction between the infected and effector cells.

The left hand side of Eq. (1a) represents the rate of change of CoV, $V(t)$. The primary four terms of right side accounts the generation rate of CoV by contaminated cells, neutralization of CoV by particular antibodies, adsorption of viral particles by healthy cells, and the common rot of viral particles. The nonspecific mucociliary removal of virions supported by a cough and other mechanisms is described by the term $a_{V1}V/(1 + a_{V2}V)$, which saturates with increasing $V(t)$ as the available capacity of these mechanisms is exhausted.

Eq. (1b) represents the rate of alert of $H(t)$. The healthy cells are produced, due to the replications of healthy and resistant, with proportional to $(H + R)$, and D . Safe cells $R(t)$ continuously loose the resistance to disease and return to their beginning touchy state (sound state) citeJoklik, which is characterized by $a_{RR}(t)$. $g_{HV}V(t)H(t)$ represents the misfortune of solid/healthy cells due to the disease. The term $b_{HF}FH$ represents transition of healthy cells into resistant state. In the same manner, Eq. (1c) is the rate of change of infected cells $I(t)$. Infection of healthy cells by virions is described in the term $\gamma_{HV}VH$. The term $a_I I$ indicates the natural death of infected cells during which new virus particles are produced. The term $b_{IE}EI$ is the destruction of infected cells by effector cells (CTL and NK) during which no new virus is produced.

Eq. (1d) shows the rate of change of activated APC ($M(t)$), which is proportional to the amount of the virus and the number of dead cells. The natural decay of activated state of APC is represented by the last term, wheres Eq. (refE) indicates that safe cells $R(t)$ are actuated from solid cells ($b_{HF}F(t)H(t)$) and change over back to solid cells ($a_{RR}(t)$) with a limited lifetime. Eq. (1f) describes the rate of change of interferon- α that depends on the production rate of $F(t)$ by APC and by infected cells, at the rate of $F(t)$ binding healthy cells, as well as on the nonspecific decay of $F(t)$.

The seventh Eq. (1g) represents the rate of alert of effector cells $E(t)$ concentration. The essential terms talks to the era rate of effector cells braced by APC, and minute term os the demolition rate of sullied cells by effector cells, $b_{EI}I(t - \tau)E(t - \tau)$. The time-lag $\tau \geq 0$ is considered to legitimize the specified time of reaction between the corrupted and effector cells. The terms $a_E(1 - E)$ and $a_P(1 - P)$ in (1g) and (refH) are expressions for homeostatic upkeep of the levels of energetic effectors and plasma cells, reflecting the discernment that the strong body tends to protect their concentrations interior contract bounds. The essential term in the eighth Eq. of (1h) talks to the sanctioning handle of plasma cells invigorated by APC.

The ninth Eq. (1i) shows the rate of variation of antibodies $A(t)$. The primary term portrays the generation rate of antibodies by plasma cells. The second terms is the neutralization rate of free viral particles by particular antibodies, and the final term is normal rot rate of A. The variable $S(t)$ within the final Eq. (refJ) addresses the closeness between antibodies and the infection strain in a person and ranges from 0 to 1 (no compatibility to maximal compatibility). Amid the course of the infection, $S(t)$ increments as plasma cells deliver antibodies progressively congruous with viral antigens. The rate of increment of $S(t)$ is $rP(1 - S)$ that estimates for two normal perceptions: (i) the increment in $S(t)$ is fortified by plasma cells and (ii) $S(t)$ cannot increment past 1. Altering the time advancement of $S(t)$, we see how the course of the malady depends on the advancement of antigenic distance.

No single natural substance or marker shows the APC in our demonstration to supply both antigen displaying and IFN creating functions. Moreover, we excluded halfway steps within the pathways: for case, we do not account for the middle steps within the production of effector cells and plasma cells such as $Th1$ and $Th2$ partner cells and B-cells. We do not consider time-delays within the propagation of cellular components; See Figure 1.

Some presumptions are considered to streamline of our information about immune system. The populaces of cells and disease are anticipated to be reliably passed on over the epithelial layer during all times. In addition, it is accepted that the rate of alter of demonstrate variable is decided by the show value of all factors. A few variables do not have extraordinarily identifiable natural partners. The advantage of using fractional-order differential equations is that they involve memory which means that if we want to compute the fractional derivative at a current state $t = t_1$ it is necessary to consider all the previous complete history from the starting point $t = t_0$ up to the point $t = t_1$. Up to our best knowledge, there have been few numbers of fractional-order viral infection models considering the dynamics of transmission and adaptive immunity in an organism.

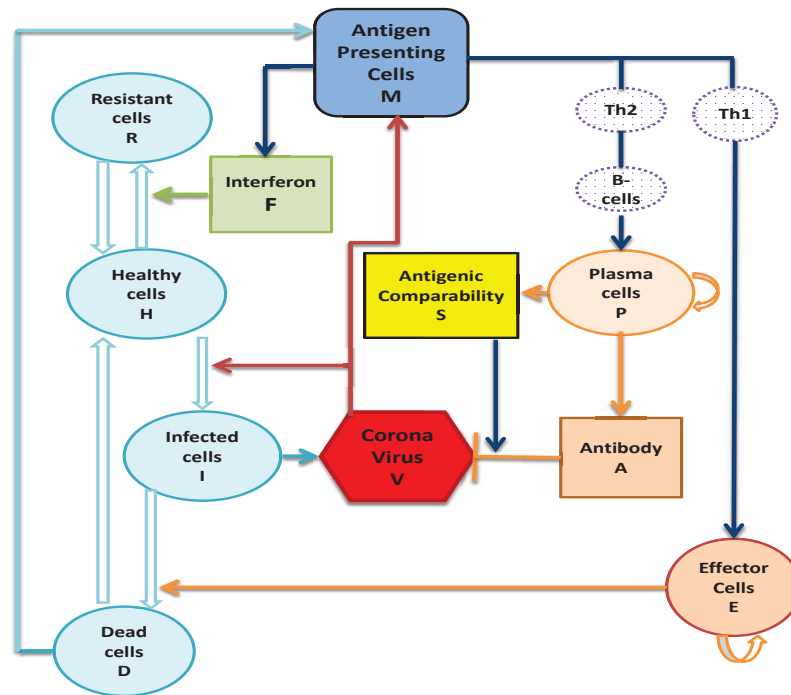


Fig. 1: Schematic representation of interactions included in model (1a-1j).

Next, we investigate the qualitative behaviour of the model through the stability of the endemic and healthy (infection-free) steady states of the above-mentioned fractional-order delay differential model.

3 Qualitative behaviours of the model

Supposing that $\mathcal{E}(V^*, H^*, I^*, M^*, F^*, R^*, E^*, P^*, A^*, S^*)$ is the steady state of system (1a-1j), and the left hand sides of the model are zeros at the steady state \mathcal{E} , one can obtain

$$\begin{aligned}
 V^* &= \frac{-\mathbf{b} \pm \sqrt{\mathbf{b}^2 - 4\mathbf{a}\mathbf{c}}}{2\mathbf{a}}, \quad H^* = \frac{b_{HD}D^*R^* + a_R R^*}{\gamma_{HV}V^* + b_{HF}F^* - b_{HD}D^*}, \quad I^* = \frac{\gamma_{HV}V^*H^*}{b_{IE}E^* + a_I}, \\
 M^* &= \frac{b_{MD}D^* + b_{MV}V^*}{b_{MD}D^* + b_{MV}V^* + a_M}, \quad F^* = \frac{b_{FM}M^* + c_F I^*}{b_{FH}H^* + a_F}, \quad R^* = \frac{b_{HF}F^*H^*}{a_R}, \\
 E^* &= \frac{a_E}{a_E + b_{EI}I^* - b_{EM}M^*}, \quad P^* = \frac{a_P}{a_P - b_{PM}M^*}, \quad A^* = \frac{b_{AP}P^*}{\gamma_{AV}S^*V^* + a_A}, \quad S^* = 1,
 \end{aligned}$$

where $\mathbf{a} = (-a_{V2}\alpha_V - a_{V2}\gamma_{VA}A^*S^* - a_{V2}\gamma_{VH}H^*)$, $\mathbf{b} = (-a_{V1} - \alpha_V V + a_{V2}\gamma_{VI}I^* - \gamma_{VA}A^*S^* - \gamma_{VH}H^*)$ and $\mathbf{c} = \gamma_V I^*$.

We call \mathcal{E}^* an endemic steady state of the model. However, a disease free or healthy steady state \mathcal{E}_0 of the model also exists,

$$\mathcal{E}_0(\cdot) = (0, 1, 0, 0, 0, 0, 1, 1, 1, 1).$$

Parameters	Narrative	Value	Sources
γ	Generation rate of CoV by contaminated cells	510	[?]
γ_A	Neutralization rate of CoV by particular antibodies	619.2	[?]
γ_{H1}	Absorption rate of CoV by infected cells	1.02	[?]
α_V	Natural decay rate of CoV	1.7	[?]
a_{V1}	Rate of nonspecific CoV removal	100	Assumed
a_{V2}	Rate of nonspecific CoV removal	23000	Assumed
b_{HD}	Rate of regeneration only occur in the presence of damage	4	[?]
a_R	Rate of cells' virus resistance state decay	1	[?]
γ_{HV}	Rate of healthy cells infected by CoV	0.34	[?]
b_{HF}	Rate of transition of healthy cells into resistant state	0.01	[?]
b_{IE}	Rate of infected cells that CTL damage	0.066	[?]
a_I	Rate of infected cells damage by cytopathicity of CoV	1.5	[?]
b_{MD}	Rate of stimulation of antigen presenting cell (APC) by dead cell	1	[?]
b_{MV}	Rate of stimulation of APC by virus	0.0037	[?]
a_M	Natural decay rate of stimulation state of APC	1	[?]
b_F	Production rate of Interferon (IFN) by APC	250000	[?]
c_F	Production rate of IFN by infected cell	2000	Assumed
b_{FH}	Rate of IFN binding healthy cells	17	[?]
a_F	Natural decay rate of IFN	8	[?]
b_{EM}	Production rate of effector cells stimulation by APC	8.3	[?]
b_{EI}	Rate of death effector cells by lytic interaction with infected cells	2.72	[?]
a_E	Natural death rate of effector cells	0.4	[?]
b_{PM}	Production rate of plasma cell	11.5	[?]
a_P	Natural death rate of plasma cell	0.4	[?]
b_A	Generation rate of counter acting agent by plasma cells	0.043	[?]
γ_{AV}	Neutralization rate of CoV by antibodies	146.2	[?]
a_A	Natural death rate of antibodies	0.043	[?]
r	Rate of S variable	$3e - 5$	Assumed

Table 1: The description and values of the parameters used in model (1a-1j).

3.1 Stability of endemic steady state \mathcal{E}^*

To investigate the stability of endemic steady state of the model (1a-1j), we linearizing the model at the steady state \mathcal{E}^* , we have

$$\begin{aligned}
 D^\beta V(t) &= (-\gamma_A S^* A^* - \gamma_{H1} H^* - \alpha_V - \frac{a_{V1}}{(1 + a_{V2} V^*)^2})V(t) - \gamma_{HV} V^* H(t) + \gamma I(t) - \gamma_A S^* V^* A(t) - \gamma_{AA} V^* S(t), \\
 D^\beta H(t) &= -\gamma_{HV} H^* V(t) + (-b_{HD}(H^* + R^*) + b_{HD}(1 - H^* - R^* - I^*) - \gamma_{HV} V^* - b_{HF} F^*)H(t) \\
 &\quad - b_{HD}(H^* + R^*)I(t) - b_{HF} H^* F(t) + (-b_{HD}(H^* + R^*) + b_{HD}(1 - H^* - R^* - I^*) + a_R)R(t), \\
 D^\beta I(t) &= \gamma_{HV} H^* V(t) + \gamma_{HV} V^* H(t) - b_{IE} E^* I(t) - a_I I(t) - b_{IE} I^* E(t), \\
 D^\beta M(t) &= b_{MV}(1 - M^*)V(t) - b_{MD}(1 - M^*)H(t) - b_{MD}(1 - M^*)I(t) \\
 &\quad - b_{MD}(1 - H^* - R^* - I^*)M(t) - b_{MV} V^* M(t) - a_M M(t) - b_{MD}(1 - M^*)R(t), \\
 D^\beta F(t) &= -b_{FH} F^* H(t) + c_F I(t) + b_F M(t) + (-b_{FH} H^* - a_F)F(t), \\
 D^\beta R(t) &= b_{HF} F^* H(t) + b_{HF} H^* F(t) - a_R R(t), \\
 D^\beta E(t) &= -b_{EI} E^* I(t - \tau) + b_{EM} E^* M(t) + (b_{EM} M^* - a_E)E(t) - b_{EI} I^* E(t - \tau), \\
 D^\beta P(t) &= b_{PM} P^* M(t) + (b_{PM} M^* - a_P)P(t), \\
 D^\beta A(t) &= -\gamma_{AV} S^* A^* V(t) + (b_A - \gamma_{AV} S^* V^* - a_A)A(t) - \gamma_{AV} V^* A^* S(t), \\
 D^\beta S(t) &= r(1 - S^*)P(t) - r P^* S(t).
 \end{aligned}
 \tag{2}$$

The vector form of (2) can be written as

$$D^\beta X(t) = \Omega X(t) + \Omega^* X(t - \tau),
 \tag{3}$$

where $X(t) = (V(t), H(t), I(t), M(t), F(t), R(t), E(t), P(t), A(t), S(t))^T$.

$$\Omega = \begin{pmatrix} \omega_1 & \omega_2 & \omega_3 & 0 & 0 & 0 & 0 & 0 & \omega_4 & \omega_5 \\ \omega_6 & \omega_7 & \omega_8 & 0 & \omega_9 & \omega_{10} & 0 & 0 & 0 & 0 \\ \omega_{11} & \omega_{12} & \omega_{13} & 0 & 0 & 0 & \omega_{14} & 0 & 0 & 0 \\ \omega_{15} & \omega_{16} & \omega_{16} & \omega_{17} & 0 & \omega_{16} & 0 & 0 & 0 & 0 \\ 0 & \omega_{18} & \omega_{19} & \omega_{20} & \omega_{21} & 0 & 0 & 0 & 0 & 0 \\ 0 & \omega_{22} & 0 & 0 & \omega_{23} & \omega_{24} & 0 & 0 & 0 & 0 \\ 0 & 0 & 0 & \omega_{25} & 0 & 0 & \omega_{26} & 0 & 0 & 0 \\ 0 & 0 & 0 & \omega_{27} & 0 & 0 & 0 & \omega_{28} & 0 & 0 \\ \omega_{29} & 0 & 0 & 0 & 0 & 0 & 0 & 0 & \omega_{30} & \omega_{31} \\ 0 & 0 & 0 & 0 & 0 & 0 & 0 & \omega_{32} & 0 & \omega_{33} \end{pmatrix},$$

and

$$\Omega^* = \begin{pmatrix} 0 & 0 & 0 & 0 & 0 & 0 & 0 & 0 & 0 & 0 \\ 0 & 0 & 0 & 0 & 0 & 0 & 0 & 0 & 0 & 0 \\ 0 & 0 & 0 & 0 & 0 & 0 & 0 & 0 & 0 & 0 \\ 0 & 0 & 0 & 0 & 0 & 0 & 0 & 0 & 0 & 0 \\ 0 & 0 & 0 & 0 & 0 & 0 & 0 & 0 & 0 & 0 \\ 0 & 0 & 0 & 0 & 0 & 0 & 0 & 0 & 0 & 0 \\ 0 & 0 & \omega_1^* & 0 & 0 & 0 & \omega_2^* & 0 & 0 & 0 \\ 0 & 0 & 0 & 0 & 0 & 0 & 0 & 0 & 0 & 0 \\ 0 & 0 & 0 & 0 & 0 & 0 & 0 & 0 & 0 & 0 \\ 0 & 0 & 0 & 0 & 0 & 0 & 0 & 0 & 0 & 0 \end{pmatrix},$$

with $\omega_1 = -\gamma_{VA}S^*A^* - \gamma_{VH}H^* - \alpha_V - \frac{a_{V1}}{(1+a_{V2}V^*)^2}$, $\omega_2 = -\gamma_{HV}V^*$, $\omega_3 = \gamma_V$, $\omega_4 = -\gamma_{VA}S^*V^*$, $\omega_5 = -\gamma_{VA}A^*V^*$, $\omega_6 = -\gamma_{HV}H^*$, $\omega_7 = (-b_{HD}(H^* + R^*) + b_{HD}(1 - H^* - R^* - I^*) - \gamma_{HV}V^* - b_{HF}F^*)$, $\omega_8 = -b_{HD}(H^* + R^*)$, $\omega_9 = -b_{HF}H^*$, $\omega_{10} = -b_{HD}(H^* + R^*) + b_{HD}(1 - H^* - R^* - I^*) + a_R$, $\omega_{11} = \gamma_{HV}H^*$, $\omega_{12} = \gamma_{HV}V^*$, $\omega_{13} = -b_{IE}E^* - a_I$, $\omega_{14} = -b_{IE}I^*$, $\omega_{15} = b_{MV}(1 - M^*)$, $\omega_{16} = -b_{MD}(1 - M^*)$, $\omega_{17} = -b_{MD}(1 - H^* - R^* - I^*) - b_{MV}V^* - a_M$, $\omega_{18} = -b_{FH}F^*$, $\omega_{19} = c_F$, $\omega_{20} = b_F$, $\omega_{21} = -b_{FH}H^* - a_F$, $\omega_{22} = b_{HF}F^*$, $\omega_{23} = b_{HF}H^*$, $\omega_{24} = -a_R$, $\omega_{25} = b_{EM}E^*$, $\omega_{26} = b_{EM}M^* - a_E$, $\omega_{27} = b_{PM}P^*$, $\omega_{28} = b_{PM}M^* - a_P$, $\omega_{29} = -\gamma_{AV}S^*A^*$, $\omega_{30} = b_A - \gamma_{AV}S^*V^* - a_A$, $\omega_{31} = -\gamma_{AV}V^*A^*$, $\omega_{32} = r(1 - S^*)$, $\omega_{33} = -rP^*$, $\omega_1^* = -b_{EI}E^*$, $\omega_2^* = -b_{EI}I^*$.

Taking Laplace transformation on both sides of (3), we have

$$s^\beta Y(s) - s^{\beta-1} \psi(0) = \Omega Y(s) + \Omega^* e^{-s\tau} \left[Y(s) + \int_{-\tau}^0 e^{-st} \psi(t) dt \right], \tag{4}$$

where $Y(s) = Y_i(s)$, $i = 1, 2, \dots, 10$, is the Laplace transform of $X(t)$, i.e. $Y(s) = \mathcal{L}(X(t))$ and $\psi(t) = \psi_i(t)$, $t \in [-\tau, 0]$, $i = 1, 2, \dots, 10$, is the initial value of the model (1a-1j). Next, we rewrite the equation (4) as

$$\Delta(s) \begin{pmatrix} Y_1(s) \\ Y_2(s) \\ \vdots \\ Y_{10}(s) \end{pmatrix} = \begin{pmatrix} d_1(s) \\ d_2(s) \\ \vdots \\ d_{10}(s) \end{pmatrix}. \tag{5}$$

Here,

$$\begin{aligned} d_1(s) &= s^{\beta-1} \psi_1(0), \quad d_2(s) = s^{\beta-1} \psi_2(0), \quad d_3(s) = s^{\beta-1} \psi_3(0), \quad d_4(s) = s^{\beta-1} \psi_4(0), \quad d_5(s) = s^{\beta-1} \psi_5(0), \\ d_6(s) &= s^{\beta-1} \psi_6(0), \quad d_7(s) = s^{\beta-1} \psi_1(0) + \omega_1^* e^{-s\tau} \int_{-\tau}^0 e^{-st} \psi_3(t) dt + \omega_2^* e^{-s\tau} \int_{-\tau}^0 e^{-st} \psi_7(t) dt, \\ d_8(s) &= s^{\beta-1} \psi_8(0), \quad d_9(s) = s^{\beta-1} \psi_9(0), \quad d_{10}(s) = s^{\beta-1} \psi_{10}(0) \end{aligned}$$

and

$$\Delta(s) = \begin{pmatrix} s_1 & -\omega_2 & -\omega_3 & 0 & 0 & 0 & 0 & 0 & -\omega_4 & -\omega_5 \\ -\omega_6 & s_2 & -\omega_8 & 0 & -\omega_9 & -\omega_{10} & 0 & 0 & 0 & 0 \\ -\omega_{11} & -\omega_{12} & s_3 & 0 & 0 & 0 & -\omega_{14} & 0 & 0 & 0 \\ -\omega_{15} & -\omega_{16} & -\omega_{16} & s_4 & 0 & -\omega_{16} & 0 & 0 & 0 & 0 \\ 0 & -\omega_{18} & -\omega_{19} & -\omega_{20} & s_5 & 0 & 0 & 0 & 0 & 0 \\ 0 & -\omega_{22} & 0 & 0 & -\omega_{23} & s_6 & 0 & 0 & 0 & 0 \\ 0 & 0 & -\omega_1^* e^{-s\tau} & -\omega_{25} & 0 & 0 & s_7 & 0 & 0 & 0 \\ 0 & 0 & 0 & -\omega_{27} & 0 & 0 & 0 & s_8 & 0 & 0 \\ -\omega_{29} & 0 & 0 & 0 & 0 & 0 & 0 & 0 & s_9 & -\omega_{31} \\ 0 & 0 & 0 & 0 & 0 & 0 & 0 & -\omega_{32} & 0 & s_{10} \end{pmatrix},$$

with $s_1 = s^\beta - \omega_1$, $s_2 = s^\beta - \omega_7$, $s_3 = s^\beta - \omega_{13}$, $s_4 = s^\beta - \omega_{17}$, $s_5 = s^\beta - \omega_{21}$, $s_6 = s^\beta - \omega_{24}$, $s_7 s^\beta - \omega_{26} - \omega_2^* e^{-s\tau}$, $s_8 = s^\beta - \omega_{28}$, $s_9 = s^\beta - \omega_{30}$, $s_{10} = s^\beta - \omega_{33}$.

Moreover, $\Delta(s)$ is known as the characteristic matrix of the model (2) and $\det(\Delta(s))$ as the characteristic polynomial of $\Delta(s)$. Sstability of the model (2) is purely obtained by the distribution of eigenvalues of $\det(\Delta(s))$.

Now, we obtain the characteristic equation of the model (3) ($\det\Delta(s) = 0$) at \mathcal{E}^* as follows:

$$P_1(s) + P_s(s)e^{-s\tau} = 0, \quad (6)$$

where

$$P_1(s) = s^{10\beta} + A_1 s^{9\beta} + A_2 s^{8\beta} + A_3 s^{7\beta} + A_4 s^{6\beta} + A_5 s^{5\beta} + A_6 s^{4\beta} + A_7 s^{3\beta} + A_8 s^{2\beta} + A_9 s^\beta + A_{10},$$

$$P_2(s) = B_1 s^{9\beta} + B_2 s^{8\beta} + B_3 s^{7\beta} + B_4 s^{6\beta} + B_5 s^{5\beta} + B_6 s^{4\beta} + B_7 s^{3\beta} + B_8 s^{2\beta} + B_9 s^\beta + B_{10},$$

and A_i ($i = 1, 2, \dots, 10$), B_j ($j = 1, 2, \dots, 9$) are constants based on the various combinations of the parameter values of given model (2). We consider the two cases:

• **Case 1:** $\tau > 0$. Herein, we prove that the characteristic equation (6) has no pure imaginary roots for any $\tau > 0$. But, let us assume that the characteristic equation (6) has pure imaginary root, i.e. $s = i\zeta = \zeta(\cos \frac{\pi}{2} + i \sin \frac{\pi}{2})$, $\zeta > 0$. Substituting the pure imaginary root s into (6), we get

$$C_1 + iD_1 + (C_2 + iD_2)e^{-i\zeta\tau} = 0, \quad (7)$$

where C_1, C_2 and D_1, D_2 are real and imaginary part of $P_1(s)$ and $P_2(s)$. Here,

$$\begin{aligned}
 C_1 &= \zeta^{10\beta} \cos(5\beta\pi) + A_1 \zeta^{9\beta} \cos\left(\frac{9\beta\pi}{2}\right) + A_2 \zeta^{8\beta} \cos(4\beta\pi) + A_3 \zeta^{7\beta} \cos\left(\frac{7\beta\pi}{2}\right) + A_4 \zeta^{6\beta} \cos(3\beta\pi) \\
 &\quad + A_5 \zeta^{5\beta} \cos\left(\frac{5\beta\pi}{2}\right) + A_6 \zeta^{4\beta} \cos(2\beta\pi) + A_7 \zeta^{3\beta} \cos\left(\frac{3\beta\pi}{2}\right) + A_8 \zeta^{2\beta} \cos(\beta\pi) \\
 &\quad + A_9 \zeta^\beta \cos\left(\frac{\beta\pi}{2}\right) + A_{10}, \\
 D_1 &= \zeta^{10\beta} \sin(5\beta\pi) + A_1 \zeta^{9\beta} \sin\left(\frac{9\beta\pi}{2}\right) + A_2 \zeta^{8\beta} \sin(4\beta\pi) + A_3 \zeta^{7\beta} \sin\left(\frac{7\beta\pi}{2}\right) + A_4 \zeta^{6\beta} \sin(3\beta\pi) \\
 &\quad + A_5 \zeta^{5\beta} \sin\left(\frac{5\beta\pi}{2}\right) + A_6 \zeta^{4\beta} \sin(2\beta\pi) + A_7 \zeta^{3\beta} \sin\left(\frac{3\beta\pi}{2}\right) + A_8 \zeta^{2\beta} \sin(\beta\pi) \\
 &\quad + A_9 \zeta^\beta \sin\left(\frac{\beta\pi}{2}\right) \\
 C_2 &= B_1 \zeta^{9\beta} \cos\left(\frac{9\beta\pi}{2}\right) + B_2 \zeta^{8\beta} \cos(4\beta\pi) + B_3 \zeta^{7\beta} \cos\left(\frac{7\beta\pi}{2}\right) + B_4 \zeta^{6\beta} \cos(3\beta\pi) \\
 &\quad + B_5 \zeta^{5\beta} \cos\left(\frac{5\beta\pi}{2}\right) + B_6 \zeta^{4\beta} \cos(2\beta\pi) + B_7 \zeta^{3\beta} \cos\left(\frac{3\beta\pi}{2}\right) + B_8 \zeta^{2\beta} \cos(\beta\pi) \\
 &\quad + B_9 \zeta^\beta \cos\left(\frac{\beta\pi}{2}\right) + B_{10}, \\
 D_2 &= B_1 \zeta^{9\beta} \sin\left(\frac{9\beta\pi}{2}\right) + B_2 \zeta^{8\beta} \sin(4\beta\pi) + B_3 \zeta^{7\beta} \sin\left(\frac{7\beta\pi}{2}\right) + B_4 \zeta^{6\beta} \sin(3\beta\pi) \\
 &\quad + B_5 \zeta^{5\beta} \sin\left(\frac{5\beta\pi}{2}\right) + B_6 \zeta^{4\beta} \sin(2\beta\pi) + B_7 \zeta^{3\beta} \sin\left(\frac{3\beta\pi}{2}\right) + B_8 \zeta^{2\beta} \sin(\beta\pi) \\
 &\quad + B_9 \zeta^\beta \sin\left(\frac{\beta\pi}{2}\right)
 \end{aligned}$$

Separating equation (7) into its real and imaginary parts, we have

$$\begin{cases} C_2 \cos \zeta \tau + D_2 \sin \zeta \tau = -C_1, \\ D_2 \cos \zeta \tau - C_2 \sin \zeta \tau = -D_1. \end{cases} \tag{8}$$

From (8),

$$\begin{cases} \cos \zeta \tau = \frac{-(C_1 C_2 + D_1 D_2)}{C_2^2 + D_2^2} = \mathbb{G}_1(\zeta), \\ \sin \zeta \tau = \frac{(C_2 D_1 - D_2 C_1)}{C_2^2 + D_2^2} = \mathbb{G}_2(\zeta). \end{cases} \tag{9}$$

Squaring and adding (9),

$$\mathbb{G}_1^2(\zeta) + \mathbb{G}_2^2(\zeta) = 1. \tag{10}$$

It follows that $\cos \zeta \tau = \mathbb{G}_1(\zeta)$, then

$$\tau^{(k)} = \frac{1}{\omega} [\arccos(\mathbb{G}_1(\zeta)) + 2k\pi], \quad k = 0, 1, 2, \dots \tag{11}$$

Hence, it is clear that equation (10) has one positive root at least. Thus, the bifurcation point is defined as

$$\tau_0 = \min\{\tau^{(k)}\}, \quad k = 0, 1, 2, \dots, \tag{12}$$

where $\tau^{(k)}$ is defined in (11).

• **Case 2:** $\tau = 0$. When $\tau = 0$, the characteristic equation (6) becomes

$$\lambda^{10} + Q_1 \lambda^9 + Q_2 \lambda^8 + Q_3 \lambda^7 + Q_4 \lambda^6 + Q_5 \lambda^5 + Q_6 \lambda^4 + Q_7 \lambda^3 + Q_8 \lambda^2 + Q_9 \lambda + Q_{10} = 0, \tag{13}$$

where Q_j , ($j = 1, 2, \dots, 10$) are constants based on the various parameter values given in the model (2). Using Routh-Hurwitz's criteria, the following conditions hold.

$$\begin{aligned}
 H_1 &= |Q_1| > 0, \quad H_2 = \begin{vmatrix} Q_1 & 1 \\ Q_3 & Q_2 \end{vmatrix} > 0, \quad H_3 = \begin{vmatrix} Q_1 & 1 & 0 \\ Q_3 & Q_2 & Q_1 \\ Q_5 & Q_4 & Q_3 \end{vmatrix} > 0, \quad H_4 = \begin{vmatrix} Q_1 & 1 & 0 & 0 \\ Q_3 & Q_2 & Q_1 & 1 \\ Q_5 & Q_4 & Q_3 & Q_2 \\ Q_7 & Q_6 & Q_5 & Q_4 \end{vmatrix} > 0, \\
 H_5 &= \begin{vmatrix} Q_1 & 1 & 0 & 0 & 0 \\ Q_3 & Q_2 & Q_1 & 1 & 0 \\ Q_5 & Q_4 & Q_3 & Q_2 & Q_1 \\ Q_7 & Q_6 & Q_5 & Q_4 & Q_3 \\ Q_9 & Q_8 & Q_7 & Q_6 & Q_5 \end{vmatrix} > 0, \quad H_6 = \begin{vmatrix} Q_1 & 1 & 0 & 0 & 0 & 0 \\ Q_3 & Q_2 & Q_1 & 1 & 0 & 0 \\ Q_5 & Q_4 & Q_3 & Q_2 & Q_1 & 1 \\ Q_7 & Q_6 & Q_5 & Q_4 & Q_3 & Q_2 \\ Q_9 & Q_8 & Q_7 & Q_6 & Q_5 & Q_4 \\ 0 & Q_{10} & Q_9 & Q_8 & Q_7 & Q_6 \end{vmatrix} > 0, \quad H_7 = \begin{vmatrix} Q_1 & 1 & 0 & 0 & 0 & 0 & 0 \\ Q_3 & Q_2 & Q_1 & 1 & 0 & 0 & 0 \\ Q_5 & Q_4 & Q_3 & Q_2 & Q_1 & 1 & 0 \\ Q_7 & Q_6 & Q_5 & Q_4 & Q_3 & Q_2 & Q_1 \\ Q_9 & Q_8 & Q_7 & Q_6 & Q_5 & Q_4 & Q_3 \\ 0 & Q_{10} & Q_9 & Q_8 & Q_7 & Q_6 & Q_5 \\ 0 & 0 & 0 & Q_{10} & Q_9 & Q_8 & Q_7 \end{vmatrix} > 0, \\
 H_8 &= \begin{vmatrix} Q_1 & 1 & 0 & 0 & 0 & 0 & 0 & 0 \\ Q_3 & Q_2 & Q_1 & 1 & 0 & 0 & 0 & 0 \\ Q_5 & Q_4 & Q_3 & Q_2 & Q_1 & 1 & 0 & 0 \\ Q_7 & Q_6 & Q_5 & Q_4 & Q_3 & Q_2 & Q_1 & 1 \\ Q_9 & Q_8 & Q_7 & Q_6 & Q_5 & Q_4 & Q_3 & Q_2 \\ 0 & Q_{10} & Q_9 & Q_8 & Q_7 & Q_6 & Q_5 & Q_4 \\ 0 & 0 & 0 & Q_{10} & Q_9 & Q_8 & Q_7 & Q_6 \\ 0 & 0 & 0 & 0 & 0 & Q_{10} & Q_9 & Q_8 \end{vmatrix} > 0, \quad H_9 = \begin{vmatrix} Q_1 & 1 & 0 & 0 & 0 & 0 & 0 & 0 & 0 \\ Q_3 & Q_2 & Q_1 & 1 & 0 & 0 & 0 & 0 & 0 \\ Q_5 & Q_4 & Q_3 & Q_2 & Q_1 & 1 & 0 & 0 & 0 \\ Q_7 & Q_6 & Q_5 & Q_4 & Q_3 & Q_2 & Q_1 & 1 & 0 \\ Q_9 & Q_8 & Q_7 & Q_6 & Q_5 & Q_4 & Q_3 & Q_2 & Q_1 \\ 0 & Q_{10} & Q_9 & Q_8 & Q_7 & Q_6 & Q_5 & Q_4 & Q_3 \\ 0 & 0 & 0 & Q_{10} & Q_9 & Q_8 & Q_7 & Q_6 & Q_5 \\ 0 & 0 & 0 & 0 & 0 & Q_{10} & Q_9 & Q_8 & Q_7 \\ 0 & 0 & 0 & 0 & 0 & 0 & 0 & Q_{10} & Q_9 \end{vmatrix} > 0, \quad H_{10} = Q_{10}H_9 > 0.
 \end{aligned}$$

Hence, the eigenvalues of the characteristic equation (13) have negative real parts. It is clear that the endemic steady state \mathcal{E}^* of the model (2) is asymptotically stable when $\tau = 0$.

Theorem 1. For any $\tau > 0$, $H_i > 0$, ($i = 1, 2, \dots, 10$) holds. Then, the endemic steady state \mathcal{E}^* of the model (1a-1j) with fractional order $\beta \in (0, 1)$ is locally asymptotically stable.

3.2 Stability of healthy steady state \mathcal{E}_0

Now, we consider healthy steady state \mathcal{E}_0^* of model (1a-1j) as

$$\mathcal{E}_h^*(\cdot) = (0, 1, 0, 0, 0, 0, 1, 1, 1, 1).$$

At the healthy steady state \mathcal{E}_0^* , system (3) is reduced as

$$D^\beta X(t) = \Omega X(t) + \Omega^* X(t - \tau), \quad (14)$$

where $X(t) = (V(t), H(t), I(t), M(t), F(t), R(t), E(t), P(t), A(t), S(t))^T$,

$$\Omega = \begin{pmatrix} \phi_1 & 0 & \phi_2 & 0 & 0 & 0 & 0 & 0 & 0 & 0 \\ \phi_3 & \phi_4 & \phi_4 & 0 & \phi_5 & \phi_6 & 0 & 0 & 0 & 0 \\ \phi_7 & 0 & \phi_8 & 0 & 0 & 0 & 0 & 0 & 0 & 0 \\ \phi_9 & \phi_{10} & \phi_{10} & \phi_{11} & 0 & \phi_{10} & 0 & 0 & 0 & 0 \\ 0 & 0 & \phi_{12} & \phi_{13} & \phi_{14} & 0 & 0 & 0 & 0 & 0 \\ 0 & 0 & 0 & 0 & \phi_{15} & \phi_{16} & 0 & 0 & 0 & 0 \\ 0 & 0 & 0 & \phi_{17} & 0 & 0 & \phi_{18} & 0 & 0 & 0 \\ 0 & 0 & 0 & \phi_{19} & 0 & 0 & 0 & \phi_{20} & 0 & 0 \\ \phi_{21} & 0 & 0 & 0 & 0 & 0 & 0 & 0 & 0 & 0 \\ 0 & 0 & 0 & 0 & 0 & 0 & 0 & 0 & 0 & \phi_{22} \end{pmatrix},$$

and

$$\Omega^* = \begin{pmatrix} 0 & 0 & 0 & 0 & 0 & 0 & 0 & 0 & 0 & 0 \\ 0 & 0 & 0 & 0 & 0 & 0 & 0 & 0 & 0 & 0 \\ 0 & 0 & 0 & 0 & 0 & 0 & 0 & 0 & 0 & 0 \\ 0 & 0 & 0 & 0 & 0 & 0 & 0 & 0 & 0 & 0 \\ 0 & 0 & 0 & 0 & 0 & 0 & 0 & 0 & 0 & 0 \\ 0 & 0 & 0 & 0 & 0 & 0 & 0 & 0 & 0 & 0 \\ 0 & 0 & \phi_1^* & 0 & 0 & 0 & 0 & 0 & 0 & 0 \\ 0 & 0 & 0 & 0 & 0 & 0 & 0 & 0 & 0 & 0 \\ 0 & 0 & 0 & 0 & 0 & 0 & 0 & 0 & 0 & 0 \\ 0 & 0 & 0 & 0 & 0 & 0 & 0 & 0 & 0 & 0 \end{pmatrix},$$

with $\phi_1 = -\gamma_{VA}S^*A^* - \gamma_{VH}H^* - \alpha_V$, $\phi_2 = \gamma_V$, $\phi_3 = -\gamma_{HV}H^*$, $\phi_4 = -b_{HD}$, $\phi_5 = -b_{HF}$, $\phi_6 = -b_{HD} + a_R$, $\phi_7 = \gamma_{HV}$, $\phi_8 = -b_{IE} - a_I$, $\phi_9 = b_{MV}$, $\phi_{10} = -b_{MD}$, $\phi_{11} = -a_M$, $\phi_{12} = c_F$, $\phi_{13} = b_F$, $\phi_{14} = -b_{FH} - a_F$, $\phi_{15} = b_{HF}$, $\phi_{16} = -a_R$, $\phi_{17} = b_{EM}E^*$, $\phi_{18} = -a_E$, $\phi_{19} = b_{PM}$, $\phi_{20} = -a_P$, $\phi_{21} = -\gamma_{AV}$, $\phi_{22} = -r$, $\phi_{23}^* = -b_{EI}$.

Now, applying the same procedure (taking Laplace transform on (14)), we find the characteristic equation $\det\Delta(s) = 0$ of system (1a-1j) at \mathcal{E}_0^* is

$$s^{10\beta} + T_1s^{9\beta} + T_2s^{8\beta} + T_3s^{7\beta} + T_4s^{6\beta} + T_5s^{5\beta} + T_6s^{4\beta} + T_7s^{3\beta} + T_8s^{2\beta} + T_9s^\beta + T_{10} = 0, \tag{15}$$

where T_j , ($j = 1, 2, \dots, 10$) are constants based on the various parameter values given in (14). According to the well-known Routh-Hurwitz criteria, the eigenvalues of (15) have negative real parts.

Theorem 2. When $\tau \geq 0$, $T_i > 0$, ($i = 1, 2, \dots, 10$) hold. Then all roots of equation (15) have negative real parts. Hence, the healthy steady state (infection-free) \mathcal{E}_0^* of system (1a-1j) is asymptotically stable.

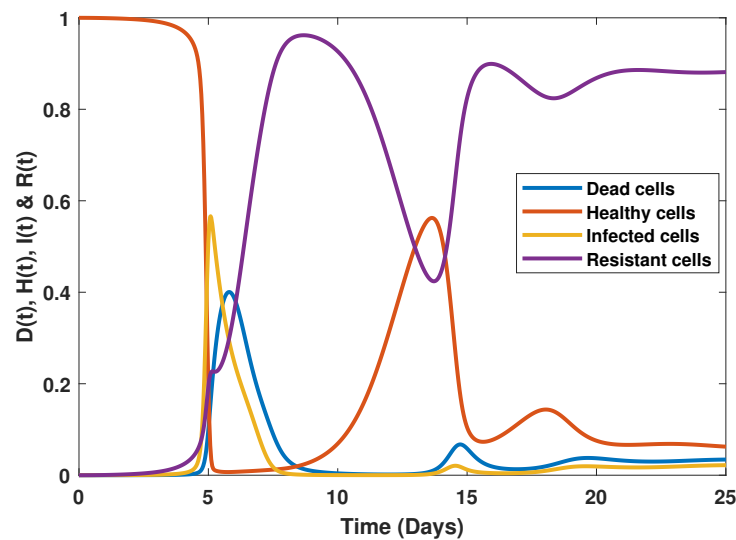


Fig. 2: Numerical simulations of proportion of Dead cells, Healthy cells, Infected cells and Resistant/Safe cells of the model (1a-1j) at $\beta = 1.0$, $\tau = 1.0$. The Figure shows a periodic outbreak due to the memory of time-delay τ .

Figure 2 demonstrates numerical simulation of four different cells (healthy cells, dead cells, Infected cells and resistant cells) of model (1a-1j) at $\beta = 1.0$, $\tau = 1.0$ and parameter values given in the Table 2. The Figure shows a periodic outbreak due to the time-delay τ . While, Figure 3 shows dynamics of the model with different values of the fractional order β ($= 1.0, 0.95, 0.9$) and time-delay $\tau = 1.0$. Figure 3 reveals that when $\beta = 1$ virus level peaks after 7-8 days. This interval increases as β decreases but with lower maximum.

We have the following Remarks.

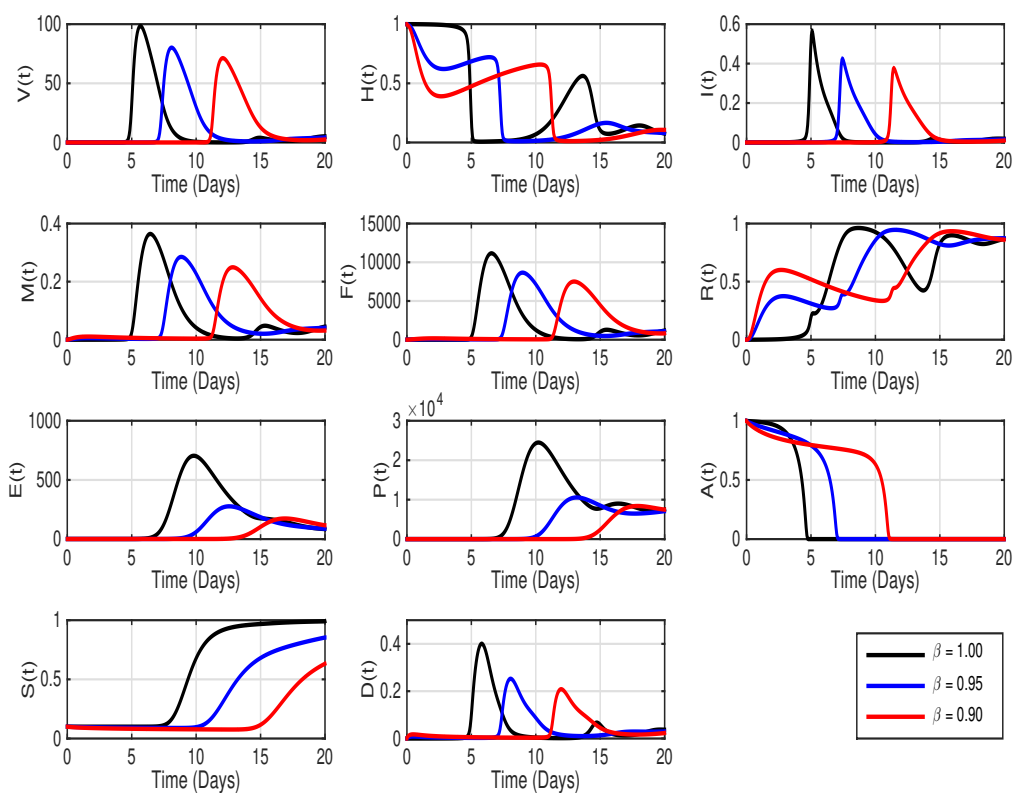


Fig. 3: The dynamics of state trajectories of the model (1a-1j) with the parameter values shown in Table 2, time-delay $\tau = 1.0$ and various values of fractional-order: $\beta = 1.0, 0.95, 0.9$. The fractional-order plays the role of long-run memory in the model.

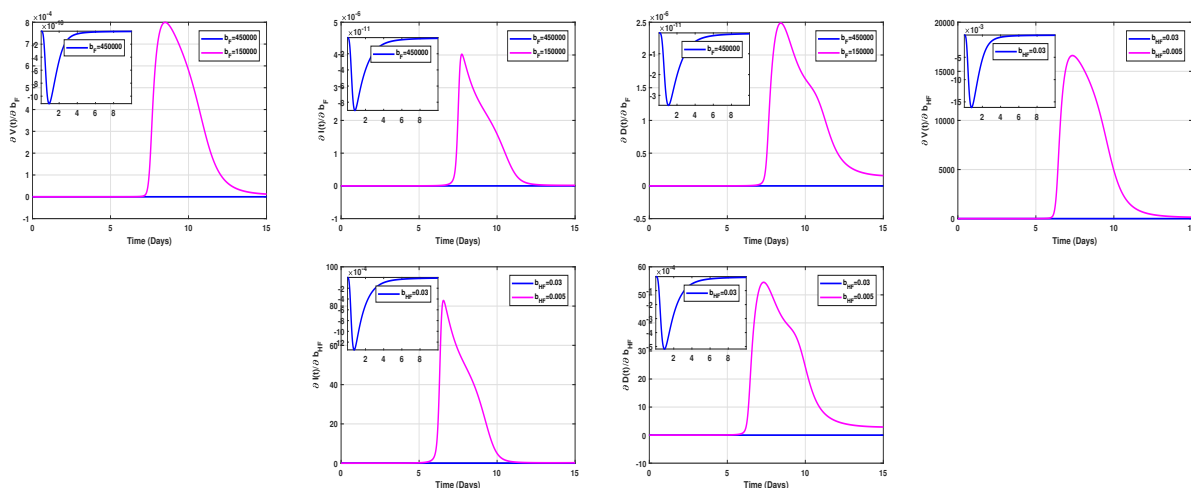


Fig. 4: Sensitivity of $V(t)$, $I(t)$ and $D(t)$ due to small changes on the interferon parameters b_F and b_{HF} . We notice that the model-states are sensitive in the first stage and with lower values of the b_F and b_{HF} , the components $V(t)$, $I(t)$ and $D(t)$ become more sensitive.

Remark. A combination of a delay-time and fractional-order in the model leads to a notable increase in the complexity of the observed behavior, as the solution is continuously based on all the previous states. However, the presence of fractional-order damps the oscillatory behaviors of the model. The fractional-order plays the role of the memory.

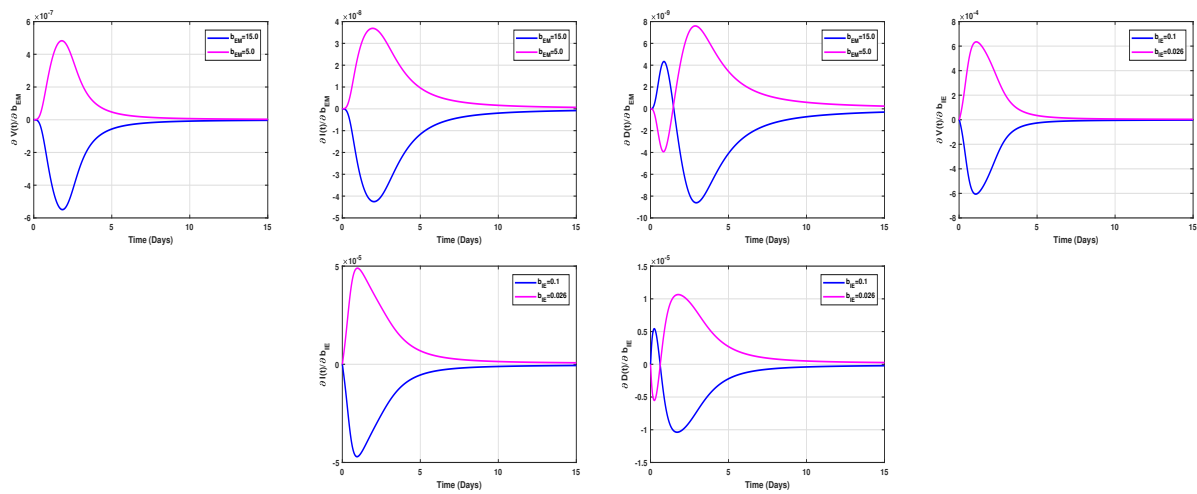


Fig. 5: This shows sensitivity of $V(t)$, $I(t)$ and $D(t)$ due to small variations on the innate immunity parameters b_{EM} and b_{IE} . We notice that the model is sensitive in the first stage. Also, the lower values of the b_{EM} and b_{IE} , the more sensitivity.

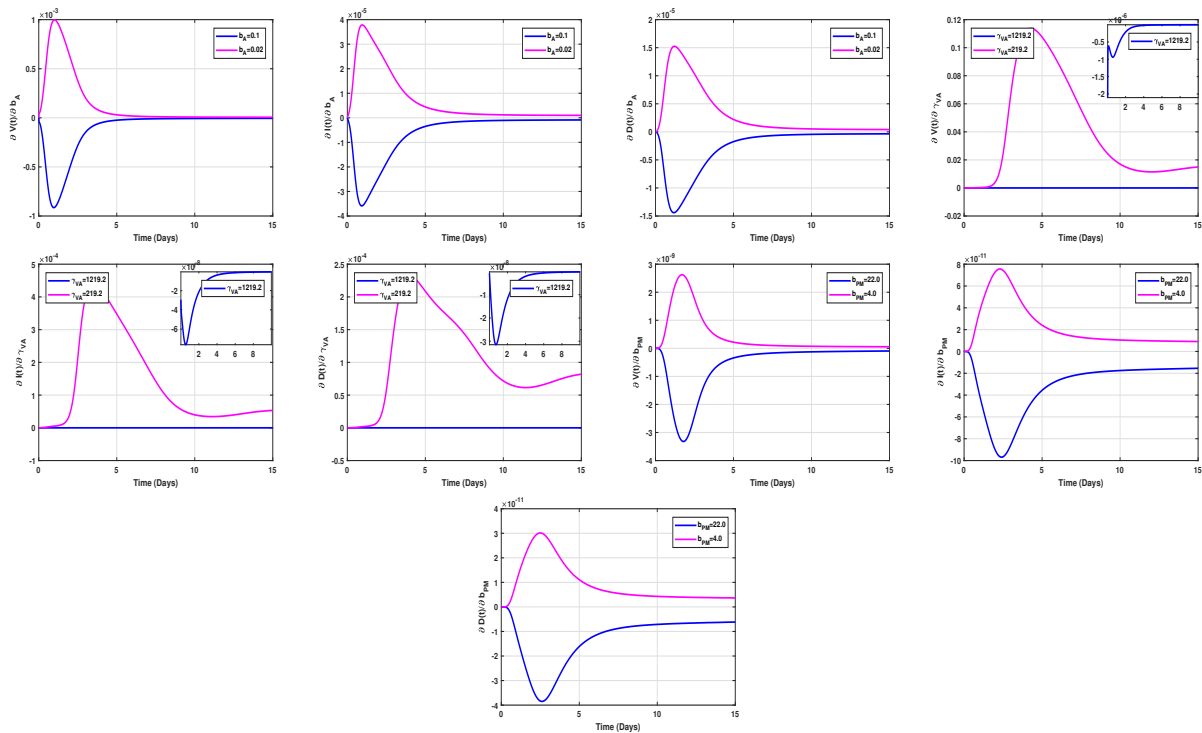


Fig. 6: This shows sensitivity of $V(t)$, $I(t)$ and $D(t)$ due to small variations on the adaptive immunity parameters b_A , b_{PM} and γ_{VA} . We notice that the model is sensitive in the first stage. Also the lower values of the b_A , b_{PM} and γ_{VA} , the more sensitivity.

Remark. The fractional derivative $\beta \in (0, 1]$ is defined by Caputo sense (See the Appendix), so introducing a convolution integral with a power-law memory kernel benefits in describing memory effects in dynamical systems. The decaying rate of the memory kernel depends on β . A lower value of α corresponding to more slowly-decaying time-correlation functions leads a long memory. Therefore, as $\beta \rightarrow 1$, the influence of memory decreases.

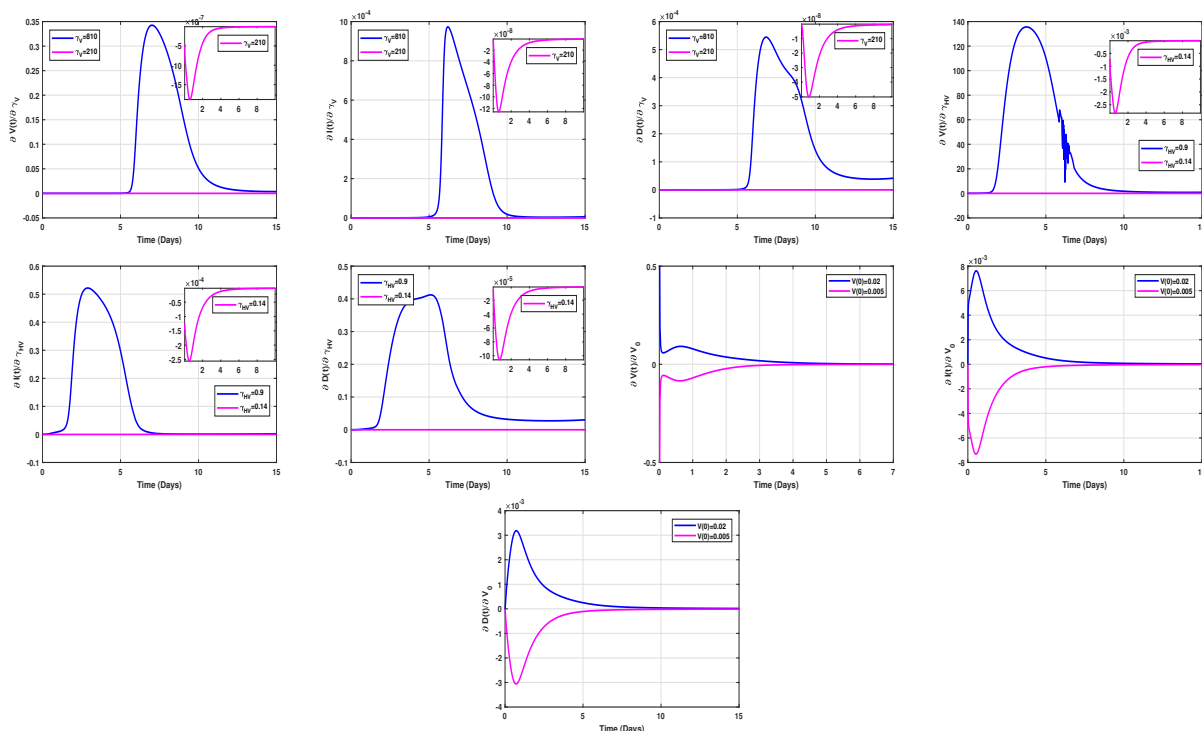


Fig. 7: Sensitivity of $V(t)$, $I(t)$ and $D(t)$ due to small variations on the pathogen parameters γ_V , γ_{VH} and $V(0)$. We notice that the model is sensitive in the first stage. However, the higher values of γ_V , γ_{VH} and $V(0)$ the more sensitivity. Sensitivity of $V(t)$ due to small changes on the initial value V_0 , rate of production of infected cells γ_V , adsorption rate of $V(t)$ by healthy cells γ_{VH} , and rate of neutralization of $V(t)$ by antibodies γ_{VA} . We notice that the viral infection is contiguously sensitive to the initial infection V_0 and the sensitivity decreases with time. The parameters γ_{VH} and γ_{VA} are very effective in the subinterval 4–10 days.

4 Sensitivity analysis

Sensitivity analysis is an important tool for assessing dynamic behavior of the underlying biological system. Herein, we evaluate sensitivity of state variables to small variations in model parameters to enable us to (i) display how robustness of the underlying infection model is to small changes in the parameter values, (ii) discover in which subinterval the model sensitive to a particular parameter to understand significant processes and immune system mechanisms. We evaluate the sensitivity functionals throughout studying the effect of changes in the parameters on the period to estimate severity of the diseases [?,45,46].

The first order sensitivity function can be approximated by finite-difference techniques. Assume that the state dependent of the underlying model is $Y(t,P) = [y_1,y_2,\dots,y_n]^T$ and $P = [p_1,p_2,\dots,p_m]^T$, then

$$\frac{\partial y_i}{\partial p_j} \approx \frac{\delta y_i}{\delta p_j} = [y_i(t,[p_1,p_2,\dots,p_j + \delta p_j,\dots,p_m]) - y_i(t,[p_1,p_2,\dots,p_j,\dots,p_m])]/\delta p_j.$$

As mentioned above, the information contained in the sensitivity analysis is useful for parameter identification, optimization, reduction of complex nonlinear models, and for experimental design and analysis. For example, if it can be observed that a particular parameter p_j has little effect on the solution, it may be possible to eliminate it, at some stage, from the modeling process.

Next, we discuss the sensitivity of model (1a-1j) due to small perturbations of (i) the production rate of interferon IFN by APC (through the evaluation of the first-order sensitivity functions such as $\partial V(t)/\partial b_F$, $\partial V(t)/\partial b_{HF}$); (ii) parameters of cellular components of innate immunity (through the evaluation of sensitivity functions such as $\partial V(t)/\partial b_{EM}$, $\partial V(t)/\partial b_{IM}$); (iii) adaptive immunity (through the evaluation of the sensitivity functions such as $\partial V(t)/\partial b_A$, $\partial V(t)/\partial b_{PM}$, $\partial V(t)/\partial b_{AV}$); and (iv) pathogen virulence (viral load) (through the evaluation of the sensitivity functions such as $\partial V(t)/\partial \gamma_V$, $\partial V(t)/\partial \gamma_{VH}$, $\partial V(t)/\partial V(0)$).

4.1 Sensitivity due to variation in the rate of interferon- α

The interferon reaction depends on the parameters b_F (the production rate of interferons) and b_{HF} (the rate of induction of resistant state in epithelial cells), respectively. When the production rate of interferon increases to the value $b_F = 450000$ from the standard value $b_F = 250000$, the host remains infectious for about 0-4 days. Likewise, when the production rate of interferon decreases to the value $b_F = 150000$ from the standard value, the host remains infectious for about 6-12 days. In both cases, the disease progresses for regular values of $V(0)$ and $S(0)$ and the only variance in the interval of the infectious period. On the other hand, when the value of b_{HF} increases, the host remains asymptomatic and when value of b_{HF} decreases, the host has higher infectious. Therefore, the virus flaking is sensitive to the amount of b_F and b_{HF} , i.e. for increasing values of b_F and b_{HF} , the virus shedding is low but a longer infectious period. When decreasing the values of b_F and b_{HF} , the damage in the host increases over 50% which may cause secondary infections or death. For high values of b_F and b_{HF} , onset of disease is the same, the duration of disease is short, and the damage is small. The host may cause death at very low values of b_F and b_{HF} , respectively. Figure 4 shows the sensitivity behavior of the model (1a-1j) with respect to the parameters b_F and b_{HF} . We may notice that a small change in b_F and b_{HF} can lead to a significant change in the load of CoV, with low and high values of the parameters.

4.2 Sensitivity to variation in the rate of innate immunity cells

The proliferation of effector cells of innate immunity depends on the parameters b_{EM} (the replication rate of effector cells) and b_{IE} (the rate of removal of infected cells by effectors), respectively. The disease may disappear without any signs based on the suitably large values of b_{EM} or b_{IE} . Similarly, the symptoms of the disease remain longer at the small values of b_{EM} or b_{IE} . Figure 5 shows the sensitivity of $V(t)$, $I(t)$ and $D(t)$ due to small perturbations on the innate immunity parameters b_{EM} and b_{IE} . We observe that the viral load and infected cells are sensitive to small changes in the parameters, in the first stage. Also, the lower values of the b_{EM} and b_{IE} , the more sensitivity. The variables $V(t)$, $I(t)$ and $D(t)$ become insensitive to the parameters b_{EM} and b_{IE} after 10 days. However, the sensitivity is in the peak during first 2-3 days (see Figure 5).

4.3 Sensitivity to variation in rate of adaptive immunity cells

The parameters b_{PM} represent the production rate of plasma cell, and b_A is the production rate of antibody by plasma cells), while γ_A represents the neutralization rate of CoV by antibodies. These parameters are involved in the activation of adaptive immune response. For high values of b_A , the onset of disease occurs later and damage in the host is minor. Also, a smaller numbers of viruses are shed at the peak of the disease and the infectious period is noticeably smaller, i.e. all values of b_A have the same duration of disease. Moreover, the disease always develops for low values of γ_A . The damage is less sensitive to the parameters b_{PM} and γ_A . The duration of disease is same for all values of b_{PM} and γ_A . The infection period is same for all values of γ_A and it affects the onset of disease alone. For sufficient large values of b_{PM} , the infection period becomes shorter. The infection can be removed without any signs in the host under the sufficiently large values of b_{PM} , b_A and γ_A . Figure 6 shows the sensitivity simulation of the model (1a-1j) based on small perturbations of the adaptive immunity parameters b_{PM} , b_A and γ_A .

4.4 Sensitivity to variation in pathogen virulence

The viral load is related to the changes in the initial values $V(0)$ and the parameters γ_{HV} and γ_V , which represent the rate of infection of epithelial cells by a CoV and the rate of CoV particles secretion per infected epithelial cell, respectively. The viruses can contaminate the healthy cells at high values of viral load and they replicate and mimic themselves in infected cells. The disease is constantly cultivating when the value of γ_{HV} is higher than the baseline value. Also, the disease approaches asymptomatic when the value of γ_{HV} is lower than the baseline value. In this case, the typical and severe disease establishments subject to viral load $V(0)$, namely $V(0)$ is small the disease holds asymptomatic. At the time of higher virulence ($\gamma_{HV}=0.9$), the damage in the host is high. The damage in the host is little when the virulence is less ($\gamma_{HV}=0.14$). In summary, infection by a virus of high virulence causes significant damage, as well as infection by a virus of little virulence may show the small damage or unseen damage to the host. On the other hand, the sensitivity analysis to γ_V is also significant and it shows the identical behavior of γ_{HV} . Based on the various values of viral load parameters γ_{HV} , γ_V , and $V(0)$, the sensitivity of the model (1a-1j) are shown in Figure 7. It shows that the disease develops when the virulence parameters γ_{HV} , γ_V , and $V(0)$ are high. The disease tends to asymptomatic when the virulence parameters γ_{HV} , γ_V , and $V(0)$ are less. The contagious days get longer when the disease develops for low virulence. The oscillation behaviour in the Figure means that the viral infection is very sensitive to small perturbation in the corresponding parameter.

5 Discussion and Conclusion

In this paper, we considered a comprehensive delayed fractional-order model for CoV infection with immune response in an individual/infected lung. We also considered components of innate immunity and adaptive immunity. We explored the characteristics and qualitative behaviours of the model, throughout stability and sensitivity analyses, which may help understand more details about disease spread and control in an individual. Using Laplace transformations and characteristics roots, some sufficient conditions have been deduced to ensure the asymptotic stability of the endemic and infection-free steady states of the model. The combination of a delay-time and fractional-order in the model can lead to a notable increase in the complexity of the observed behavior, as the solution continuously depends on all the previous states. The fractional-order models extend the concepts of differentiability and incorporate non-local and system memory effects through fractional-order time derivatives. The fractional-order plays the role of memory in the model. The time-lag $\tau > 0$ has been incorporated in the model to represent required time for reaction between the infected and effector cells. Some numerical simulations, using Adams-Bashforth-Moulton predictor-corrector scheme, have been shown to authenticate the derived results.

Sensitivity analysis of the model has been presented with respect to feasible parameter values and initial conditions. The oscillation behavior, in Figures 4–7, means that the viral load population is sensitive to small variations in the existing parameters. We notice that the infection occurs in an individual at the time of the changeover of healthy or chronic cells. The disease is divided into three types: (i) asymptomatic disease, (ii) typical disease, and (iii) severe disease. The asymptomatic disease occurs when the viral load is small as well as it drops monotonically to zero and the damage is also trivial. The viral inoculum stays within the certain interval may cause typical disease. However, the severe disease occurs when the viral inoculum is sufficiently large and also increases the viral load and creates the maximum damage which causes death.

Moreover, the viral load of CoV infection depends on the parameters γ_{HV} and γ_V , the rate of disease of epithelial cells by a CoV and the rate of CoV particles secretion per infected epithelial cell, respectively. For large values of γ_{HV} and γ_V , the infection may explore substantial damage. For low values of γ_{HV} and γ_V , the infection approaches asymptomatic with less damage. However, the innate immunity depends on the parameters b_F , b_{HF} , b_{EM} , and b_{IE} respectively. We may notice that a small change in these parameters can lead to a significant change in the levels of viral load, and infected cells. The infection may be cleared without any symptoms with suitably large values of b_{EM} , and b_{IE} . If the values of b_{EM} , and b_{IE} are low, the infection lasts longer. In the innate immunity, the infection is not fully cleared and the minor levels of virus inoculum are in a chronic state. On the other hand, the adaptive immunity depends on the parameters b_{PM} , b_A , and γ_{VA} respectively. The adaptive immunity has designated to remove the CoV infection in an individual in the absence of an innate immunity.

Thus, applying fractional-order to model the behavior of cells and tissues, we can begin to unravel the inherent complexity of individual molecules and membranes in a way that leads to a better understanding of the overall biological function and behavior of living systems. The results demonstrated that the combination of fractional-order derivative and time-delay in the model improved the dynamics and increased complexity of the model. Periodic outbreak of the disease can also occur due to the memory coming from time-delay τ and fractional-order. Future reserach will consider more sophisticated model with control variables to define the best strategy to treat, control and eliminate CoV infection.

Appendix

In this section, the authors present some necessary definitions and lemmas of fractional calculus, which can be used to obtain our key results.

Definition 1.[47]. The fractional integral of order β for a function u is defined as

$$I^\beta u(t) = \frac{1}{\Gamma(\beta)} \int_0^t (t-\tau)^{\beta-1} f(\tau) d\tau, \quad (16)$$

where $t \geq 0$ and $\beta > 0$, $\Gamma(\cdot)$ is the gamma function defined as $\Gamma(\beta) = \int_0^\infty t^{\beta-1} e^{-t} dt$.

Definition 2.[48]. The Caputo fractional derivative of order β for a function $u \in C^{n+1}([0, \infty), \mathbb{R})$ (the set of all $n+1$ order continuous differentiable functions on $[0, \infty)$, where \mathbb{R} denotes Euclidean space) is defined by

$${}^C_0 D_t^\beta u(t) = \frac{1}{\Gamma(n-\beta)} \int_0^t \frac{u^{(n)}(\xi)}{(t-\xi)^{\beta-n+1}} d\xi, \quad (17)$$

where $t > 0$ and n is a positive integer such that $n-1 < \beta < n \in \mathbb{Z}^+$.

The key advantage of the Caputo derivative is that it only requires that the initial conditions are given in terms of integer-order derivatives. Based on the enhancement, we use the Caputo fractional-order derivative in this paper.

Definition 3.[48]. *The Laplace transform of the Caputo fractional-order derivative is*

$$L\{ {}_0^C D_t^\beta u(t); s \} = s^\beta U(s) - \sum_{k=0}^{n-1} s^{\beta-k-1} u^{(k)}(0), \quad n-1 < \beta \leq n,$$

where $U(s)$ is the Laplace transform of $u(t)$, $u^{(k)}(0)$, $k = 1, 2, \dots, n$, are the initial conditions. If $u^{(k)}(0) = 0$, $k = 1, 2, \dots, n$, then

$$L\{ {}_0^C D_t^\beta u(t); s \} = s^\beta U(s).$$

Theorem 3.[49] *If all the roots of characteristic equation $\det(\Delta(s)) = 0$ have negative real parts, then the zero solution of system (1a-1k) is Lyapunov asymptotically stable.*

Theorem 4.[49] *If $\beta \in (0, 1)$, all the eigenvalues of $\Delta(s)$ satisfy $|\arg(s)| > \frac{\beta\pi}{2}$ and the characteristic equation $\det(\Delta(s)) = 0$ has no pure imaginary roots for $\tau_{pq} > 0$, then the zero solution of system (1a-1k) is Lyapunov asymptotically stable.*

Introducing a convolution integral with a power-law memory kernel is useful to describe memory effects in dynamical systems.

Acknowledgement

This research is funded by UAE University (Fund Code: G00003440-UPAR 2021). The authors would like to thank Professor Amr Amin (UAE University) and editor Professor Dumitru Baleanu for their valuable comments, which improved the manuscript.

References

- [1] O. Diekmann, H. Heesterbeek and T. Britton, *Mathematical tools for understanding infectious disease dynamics*, Princeton University Press, 2012.
- [2] A. Grifoni, D. Weiskopf, and et al., Targets of T Cell responses to SARS-CoV-2 coronavirus in humans with COVID-19 Disease and Unexposed Individuals, *Cell* **181**, 1?13 (2020).
- [3] F. A. Rihan, H. J. Alsakaji and C. Rajivganthi, Stochastic SIRC epidemic model with time-delay for COVID-19, *Adv. Differ. Equ.* **2020**(502),1?20 (2020).
- [4] WHO, Report of the WHO-China joint mission on coronavirus disease 2019 (COVID-19), World Health Organization, 2020.
- [5] R. M. Anderson and R. May, *Infectious diseases of humans: dynamics and control*, Oxford, OUP, 1991.
- [6] G. Marchuk, *Mathematical modelling of immune response in infectious diseases*, Dordrecht, Kluwer Academic Publishers, 1997.
- [7] C. I Siettos and L. Russo, Mathematical modeling of infectious disease dynamics, *Virulence*, **4**(4), 295?306 (2013).
- [8] W. Liu, H. W. Hethcote and S. A Levin, Dynamical behavior of epidemiological models with nonlinear incidence rates, *J. Math. Biol.* **25**(4), 359?380 (1987).
- [9] S.A Levin, B. Grenfell, A. Hastings and A. S. Perelson, Mathematical and computational challenges in population biology and ecosystems science, *Science* **275**(5298), 334?343 (1997).
- [10] A. S. Perelson, Modelling viral and immune system dynamics, *Nat. Rev. Immunol.* **2**(1), 28?36 (2002).
- [11] A. S. Perelson and P. W. Nelson, Mathematical analysis of HIV-1 dynamics in vivo, *SIAM Rev.* **41**(1), 3?44 (1999).
- [12] V. M. Zdanov and A. G. Bukrinskaja, *Myxoviruses reproduction*, Medicina, Moscow, Russia, 1969.
- [13] G. A. Marchuk, R. V. Petrov, A. A. Romanyukha and G. A. Bocharov, Mathematical model of antiviral immune response i: Data analysis, generalized picture construction and parameter evaluation for hepatitis-b, *J. Theor. Biol.* **151**, 1?40 (1991).
- [14] G. A. Bocharov and A. A. Romanyukha, Mathematical model of antiviral immune response III: influenza-a virus infection, *J. Theor. Biol.* **167**,323?360, 1994.
- [15] B. Hancioglu, D. Swigon and G. Clermont, A dynamical model of human immune response to influenza a virus infection, *J. Theor. Biol.* **246**(1), 70?86 (2007).
- [16] E. N. Wiah, I. K. Dontwi and I. A. Adetunde, Using mathematical model to depict the immune response to hepatitis b virus infection, *J. Math. Res.* **3**(2), 157-162 (2011).
- [17] E.M. Ahmed and H.A. El-Saka, On a fractional order study of middle east respiratory syndrome corona virus (mers-cov), *J. Fract. Calc. Appl.* **8**(1), 118?126 (2017).

- [18] B. Yong and L. Owen, Dynamical transmission model of MERS-CoV in two areas, In AIP Conference Proceedings, volume 1716, pages 020010?1?020010?7, AIP Publishing, 2016.
- [19] J. Lee, G. Chowell and E. Jung, A dynamic compartmental model for the middle east respiratory syndrome outbreak in the Republic of Korea: A retrospective analysis on control interventions and superspreading events, *J. Theor. Biol.* **408**, 118?126 (2016).
- [20] R. Rakkiyappan, A. Chandrasekar, F. A. Rihan and S. Lakshmanan, Exponential state estimation of Markovian jumping genetic regulatory networks with mode-dependent probabilistic time-varying delays, *Math. Bios.* **25**(1), 30?53 (2014).
- [21] R. Rakkiyappan, V. Preethi Latha and F. A. Rihan, A fractional-order model for Zika virus infection with multiple delays, *Complexity Article ID 4178073*, 20 pages (2019).
- [22] R. Chinnathamb, F. A. Rihan and H. J. Alsakaji, A fractional-order model with time delay for tuberculosis with endogenous reactivation and exogenous reinfections, *Math. Models Methods Appl. Sci.* **5**, 1?20 (2019).
- [23] F. A. Rihan, Q. Al-Mdallal, H. J. AlSakaji and A. Hashish, A fractional-order epidemic model with time-delay and nonlinear incidence rate, *Chaos Solit. Fract.* **126**, 97?105 (2019).
- [24] F. A. Rihan, S. Lakshmanan, A. H. Hashish, R. Rakkiyappan and E. Ahmed, Fractional-order delayed predator-prey systems with Holling type-II functional response. *Nonlinear Dyn.* **80**(1-2), 777?789 (2015).
- [25] F. A. Rihan, A. Hashish, F. Al-Maskari, M. S. Hussein, E. Ahmed, et al., Dynamics of tumor-immune system with fractional-order, *J. Tumor. Res.* **2**(1), 109?1?109?6 (2016).
- [26] V. P. Latha, F. A. Rihan, R. Rakkiyappan and G. Velmurugan, A fractional-order delay differential model for Ebola infection and cd8+ t-cells response: Stability analysis and Hopf bifurcation, *Int. J. Biomath.* **10**(08), 1750111?1?1750111?22 (2017).
- [27] F. Haq, K. Shah, G. Rahman and M. Shahzad, Numerical analysis of fractional order model of HIV-1 infection of cd4+ t-cells, *Numer. Meth. Part. Differ. Equ.* **5**(1), 1?11 (2017).
- [28] V. P. Latha, F. A. Rihan, R. Rakkiyappan and G. Velmurugan, A fractional-order model for Ebola virus infection with delayed immune response on heterogeneous complex networks, *J. Comput. Appl. Math.* <https://doi.org/10.1016/j.cam.2017.11.032>, 2017.
- [29] F. A. Rihan, M. Sheek-Hussein, A. Tridane and R. Yafia, Dynamics of hepatitis c virus infection: Mathematical modeling and parameter estimation, *Math. Model. Nat. Phenom.* **12**(5), 33?47 (2017).
- [30] F. A. Rihan and G. Velmurugan, Dynamics of fractional-order delay differential model for tumor-immune system, *Chaos Solit. Fract.* **132**(March):109592, (2020).
- [31] S. Arshad, D. Baleanu, J. Huang, Y. Tang and M. M. Al Qurashi, Dynamical analysis of fractional order model of immunogenic tumors, *Adv. Mech. Eng.* **8**(7), 16878140-16656704, (2016).
- [32] A. Iwasaki and R. Medzhitov, Control of adaptive immunity by the innate immune system, *Nat. Immunol.* **16**(4),343?353 (2015).
- [33] F. A. Rihan, D. H. Abdel-Rahman, S. Lakshmanan and A.S. Alkhajeh, A time delay model of tumour-immune system interactions: Global dynamics, parameter estimation, sensitivity analysis, *Appl. Math. Comput.* **232**,606?623 (2014).
- [34] F. A. Rihan and B. F Rihan, Numerical modelling of biological systems with memory using delay differential equations, *Appl. Math. Inf. Sci.* **9**(3),1645?1658 (2015).
- [35] S. Akira, S. Uemasu and O. Takeuchi, Pathogen recognition and innate immunity, *Cell* **124**(4),783?801 (2006).
- [36] B. Finlay and G. McFadden, Anti-immunology: evasion of the host immune system by bacterial and viral pathogens, *Cell* **124**(4), 767?782 (2006).
- [37] L. Zinzula and E. Tramontano, Strategies of highly pathogenic rna viruses to block dsrna detection by rig-i-like receptors: hide, mask, hit, *Antivir. Res.* **100**(3), 615?635 (2013).
- [38] D. Marc, Influenza virus non-structural protein ns1: interferon antagonism and beyond, *J. Gen. Virol.* **95**(12), 2594?2611 (2014).
- [39] J. R. Rodriguez-Madoz, A. Belicha-Villanueva, D. Bernal-Rubio, J. Ashour, J. Ayllon and A. Fernandez-Sesma, Inhibition of the type i interferon response in human dendritic cells by dengue virus infection requires a catalytically active ns2b3 complex, *J. Virol.* **84**(19), 9760?9774 (2010).
- [40] E. Kindler, H. Jonsdottir, D. Muth, O. Hamming, R. Hartmann, R. Rodriguez, R. Geffers, R. Fouchier, C. Drosten, M. Muller, et al. Efficient replication of the novel human betacoronavirus emc on primary human epithelium highlights its zoonotic potential, *MBio* **4**(1), e00611?12 (2013).
- [41] F. Zielecki, M. Weber, M. Eickmann, L. Spiegelberg, A. Zaki, M. Matrosovich, S. Becker and F. Weber, Human cell tropism and innate immune system interactions of human respiratory coronavirus emc compared to those of severe acute respiratory syndrome coronavirus, *J. Virol.* **87**(9),5300?5304 (2013).
- [42] R. W. Chan, M. C. Chan, S. Agnihothram, L. L. Chan, D. I. Kuok, J. H. Fong, Y. Guan, L. M. Poon, R. S. Baric, J. M. Nicholls, et al, Tropism of and innate immune responses to the novel human betacoronavirus lineage c virus in human ex vivo respiratory organ cultures, *J. Virol.* **87**(12), 6604?6614 (2013).
- [43] A. Dandekar and S. Perlman, Immunopathogenesis of coronavirus infections: implications for sars, *Nat. Rev. Immunol.* **5**(12), 917?927 (2005).
- [44] K. P. Keenan, J. W. Combs and E. M. McDowell, Regeneration of hamster tracheal epithelium after mechanical injury, *Virchows Arch. B Cell Pathol. Incl. Mol. Pathol.* **41**(1),193?214 (1982).
- [45] F. A. Rihan, Sensitivity analysis of dynamic systems with time lags, *J. Comput. Appl. Math.* **151**, 445?462 (2003).
- [45] F. A. Rihan, A. A. Azamov and H. J. Al-Sakaji. An inverse problem for delay differential equations: Parameter estimation, nonlinearity, sensitivity. *Appl. Math. Inf. Sci.* **12**(1),63?74 (2018).
- [46] F. A. Rihan and D. H. Abdelrahman, Sensitivity of best-fit parameters in neutral differential equations with cell growth dynamics, *Int. J. Appl. Math. Comput. Sci.* **10**,65?78 (2011).
- [47] I. Podlubny, *Fractional differential equations*, Academic Press, 1999.

- [48] H. Wang, Y. Yu and G Wen, Stability analysis of fractional-order hopfield neural networks with time delays, *Neural Netw.* **55**,98?109, (2014).
- [49] W. Deng, C. Li and J. Lu, Stability analysis of linear fractional differential system with multiple time delays, *Nonlinear Dyn.* **48**(4),409?416 (2017)
-